Electronic Supplementary Material (ESI) for Journal of Materials Chemistry C.

Supporting Information

Intensive Emission of Eu(III) β-Diketonate Complexes with Arsine Oxide Ligands

Haruki Shimoji,[a] Toshiki Fujii, [a] Akifumi Sumida [a], Yuichi Kitagawa,[bc] Yasuchika Hasegawa,[bc] Hiroaki Imoto,*[a,d] Kensuke Naka*[a,e]

[a] Faculty of Molecular Chemistry and Engineering, Graduate School of Science and Technology, Kyoto Institute of Technology, Goshokaido-cho, Matsugasaki, Sakyo-ku, Kyoto 606-8585, Japan.
[b] Faculty of Engineering, Hokkaido University, Kita-ku, Sapporo, Hokkaido 060-8628, Japan.
[c] Institute for Chemical Reaction Design and Discovery (WPI-ICReDD), Hokkaido University, Sapporo, Hokkaido 001-0021, Japan.
[d] FOREST, JST, Honcho 4-1-8, Kawaguchi, Saitama 332-0012, Japan.
[e] Materials Innovation Lab, Kyoto Institute of Technology, Goshokaido-cho, Matsugasaki, Sakyo-ku, Kyoto 606-8585, Japan.

Table of Contents

1. FT-IR spectroscopy

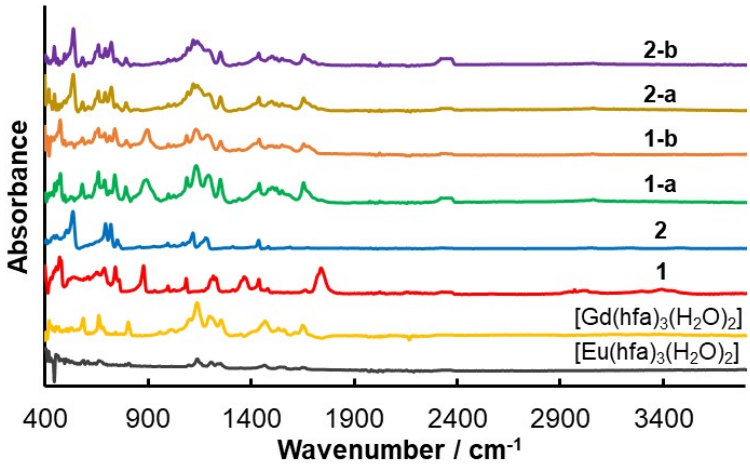

Figure S1. FT-IR analysis of $[Eu(hfa)_3(H_2O)_2]$, $[Gd(hfa)_3(H_2O)_2]$, **1**, **2**, **1-a**, **1-b**, **2-a**, and **2-b** in the solid state.

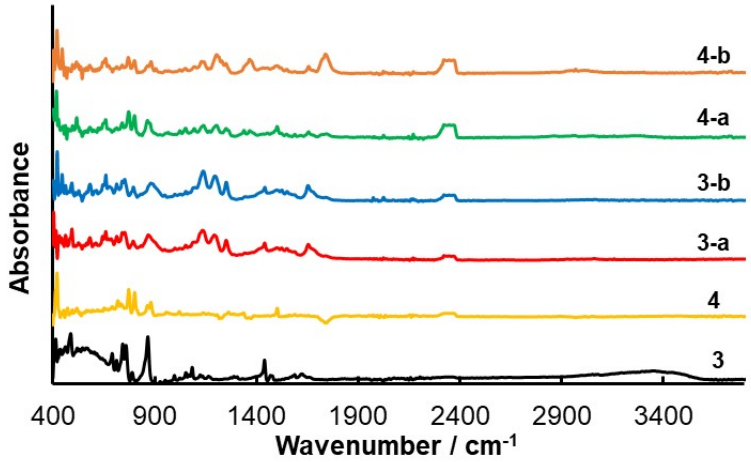

Figure S2. FT-IR analysis of **3**, **4**, **3-a**, **3-b**, **4-a**, and **4-b** in the solid state.

2. Crystallographic data

Table S1. Crystallographic data of **1-a** and **1-b**.

	1-a	**1-b**
Crystal data		
Experimental Formula	$C_{51}H_{33}As_2EuF_{18}O_8$	$C_{51}H_{33}As_2F_{18}GdO_8$
Formula Weight	1417.57	1422.86
Crystal Dimension, mm^3	0.170 × 0.270 × 0.490	0.150 × 0.170 × 0.470
Crystal System	monoclinic	monoclinic
Space Group	*P*21/*c*	*P*21/*c*
a, Å	12.7255(5)	13.0344(7)
b, Å	13.5456(5)	13.6783(6)
c, Å	30.675(1)	31.125(1)
α, deg	90.0000	90.0000
β, deg	90.986(3)	90.629(5)
γ, deg	90.0000	90.0000
Volume, $Å^3$	5286.9(4)	5548.9(5)
D_{calcd}, g cm^{-3}	1.781	1.703
Z	4	4
F(000)	2776.00	2780.00
Data Collection		
Temperature, deg	-180	20
$2\theta_{max}$, deg	52.7	52.7
Refinement		
No. of Observed Data	10792	23641
No. of Parameters	743	749
R1[a], wR2[b]	0.0341, 0.0755	0.0447, 0.1157
Goodness of Fit Indicator	1.046	1.010

[a]$R1 = \Sigma \mid |Fo| - |Fc| \mid / \Sigma |Fo|$ [b]$wR2 = [\ \Sigma w ((Fo^2-Fc^2)^2 / \Sigma w (Fo^2)^2\ ]^{1/2}$ $w = [\ \sigma^2(Fo^2)\ ]^{-1}$

CCDC #2291951 (**1-a**) and 2291952 (**1-b**)

Table S2. Crystallographic data of **2-a** and **2-b**.

	2-a	**2-b**
Crystal data		
Experimental Formula	$C_{51}H_{33}EuF_{18}O_8P_2$	$C_{51}H_{33}F_{18}GdO_8P_2$
Formula Weight	1329.67	1334.96
Crystal Dimension, mm^3	0.240 × 0.250 × 0.290	0.470 × 0.250 × 0.0740
Crystal System	monoclinic	monoclinic
Space Group	*P*21/*n*	*P*21/*n*
a, Å	17.0440(6)	17.0486(5)
b, Å	15.4405(6)	15.4596(5)
c, Å	20.6857(7)	20.7385(7)
α, deg	90.0000	90.0000
β, deg	93.952(3)	94.033(3)
γ, deg	90.0000	90.0000
Volume, $Å^3$	5430.9(3)	5452.4(3)
D_{calcd}, g cm^{-3}	1.626	1.626
Z	4	4
F(000)	2632.00	2636.00
Data Collection		
Temperature, deg	-180	-180
$2\theta_{max}$, deg	52.7	52.7
Refinement		
No. of Observed Data	11112	11153
No. of Parameters	721	721
R1[a], wR2[b]	0.0479, 0.1354	0.0347, 0.0892
Goodness of Fit Indicator	1.143	1.096

[a]$R1 = \Sigma \mid |Fo| - |Fc| \mid / \Sigma |Fo|$ [b]$wR2 = [\ \Sigma w ((Fo^2-Fc^2)^2 / \Sigma w (Fo^2)^2\ ]^{1/2}$ $w = [\ \sigma^2(Fo^2)\ ]^{-1}$

CCDC #2291953 (**2-a**) and 2291954 (**2-b**)

Table S3. Crystallographic data of **3-a** and **3-b**.

	3-a	**3-b**
Crystal data		
Experimental Formula	$C_{51.50}H_{29.50}As_2Cl_{1.50}EuF_{18}O_8$	$C_{51}H_{29}As_2GdF_{18}O_8$
Formula Weight	1473.22	1418.83
Crystal Dimension, mm^3	0.310 × 0.290 × 0.220	0.820 × 0.610 × 0.380
Crystal System	monoclinic	monoclinic
Space Group	*P*21/*n*	*P*21/*n*
a, Å	12.6740(5)	21.414(2)
b, Å	34.170(1)	12.1465(5)
c, Å	12.9216(5)	23.018(1)
α, deg	90.0000	90.0000
β, deg	91.548(3)	113.887(8)
γ, deg	90.0000	90.0000
Volume, $Å^3$	5593.9(4)	5474.1(6)
D_{calcd}, g cm^{-3}	1.749	1.722
Z	4	4
F(000)	2876.00	2764.00
Data Collection		
Temperature, deg	-180	-180
$2\theta_{max}$, deg	52.7	52.7
Refinement		
No. of Observed Data	11423	11177
No. of Parameters	758	792
R1[a], wR2[b]	0.0423, 0.1101	0.0444, 0.1049
Goodness of Fit Indicator	1.039	1.018

[a]$R1 = \Sigma \mid |Fo| - |Fc| \mid / \Sigma |Fo|$ [b]$wR2 = [\ \Sigma w ((Fo^2-Fc^2)^2 / \Sigma w (Fo^2)^2\ ]^{1/2}$ $w = [\ \sigma^2(Fo^2)\ ]^{-1}$

CCDC #2291955 (**3-a**) and 2291956 (**3-b**)

Table S4. Crystallographic data of **4-a** and **4-b**.

	4-a	**4-b**
Crystal data		
Experimental Formula	$C_{75.33}H_{45.67}As_2Cl_{0.67}EuF_{18}O_8$	$C_{76}H_{47}As_2Cl_2F_{18}GdO_8$
Formula Weight	1746.21	1808.12
Crystal Dimension, mm^3	0.320 × 0.260 × 0.160	0.250 × 0.200 × 0.0930
Crystal System	orthorhombic	orthorhombic
Space Group	*Pbca*	*Pbca*
a, Å	23.5499(8)	23.5630(8)
b, Å	20.8456(8)	20.8927(9)
c, Å	28.236(1)	28.322(1)
α, deg	90.0000	90.0000
β, deg	90.0000	90.0000
γ, deg	90.0000	90.0000
Volume, $Å^3$	13861.2(9)	13942.6(9)
D_{calcd}, g cm^{-3}	1.674	1.723
Z	8	8
F(000)	6912.00	7144.00
Data Collection		
Temperature, deg	-180	-180
$2\theta_{max}$, deg	65.4	52.7
Refinement		
No. of Observed Data	23554	14240
No. of Parameters	992	964
R1[a], wR2[b]	0.0595, 0.1189	0.0457, 0.1269
Goodness of Fit Indicator	1.189	1.053

[a]$R1 = \Sigma \mid |Fo| - |Fc| \mid / \Sigma |Fo|$ [b]$wR2 = [\ \Sigma w ((Fo^2-Fc^2)^2 / \Sigma w (Fo^2)^2\ ]^{1/2}$ $w = [\ \sigma^2(Fo^2)\ ]^{-1}$

CCDC #2291957 (**4-a**) and 2291958 (**4-b**)

Table S5. ORTEP drawing (ellipsoids at 50% probability), selected distances (Å) of **1-a** at 93 K. All hydrogens of the ligands were omitted for clarity.

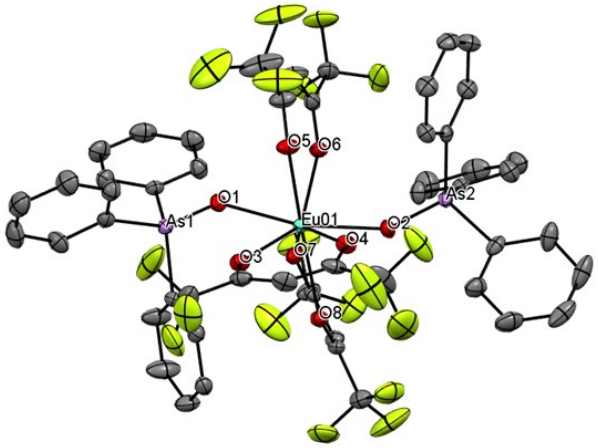

	Distance (Å)
Arsine oxide	
Eu(1) – O(1)	2.293(2)
Eu(1) – O(2)	2.283(2)
Hfa	
Eu(1) – O(3)	2.425(2)
Eu(1) – O(4)	2.438(3)
Eu(1) – O(5)	2.402(2)
Eu(1) – O(6)	2.428(2)
Eu(1) – O(7)	2.443(2)
Eu(1) – O(8)	2.427(2)

Table S6. ORTEP drawing (ellipsoids at 50% probability), selected distances (Å) of **1-b** at 293 K. All hydrogens of the ligands were omitted for clarity.

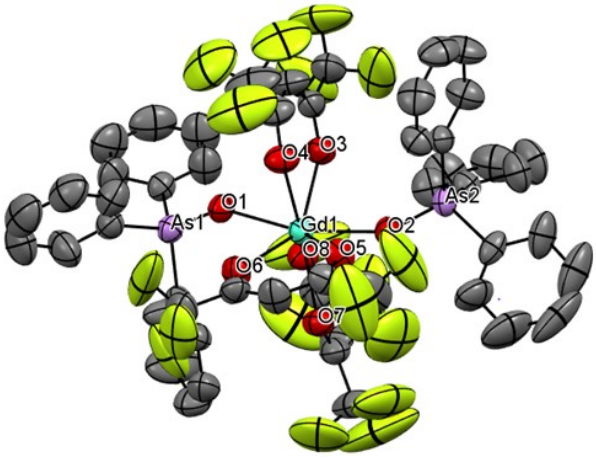

	Distance (Å)
Arsine oxide	
Gd(1) – O(1)	2.289(3)
Gd(1) – O(2)	2.274(3)
Hfa	
Gd(1) – O(3)	2.423(4)
Gd(1) – O(4)	2.380(4)
Gd(1) – O(5)	2.428(4)
Gd(1) – O(6)	2.419(4)
Gd(1) – O(7)	2405(4)
Gd(1) – O(8)	2.438(4)

Table S7. ORTEP drawing (ellipsoids at 50% probability), selected distances (Å) of **2-a** at 93 K. All hydrogens of the ligands were omitted for clarity.

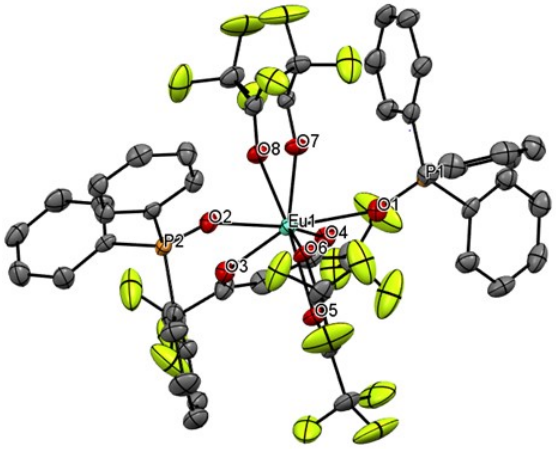

	Distance (Å)
Arsine oxide	
Eu(1) – O(1)	2.308(3)
Eu(1) – O(2)	2.307(3)
Hfa	
Eu(1) – O(3)	2.426(3)
Eu(1) – O(4)	2.422(3)
Eu(1) – O(5)	2.371(3)
Eu(1) – O(6)	2.449(3)
Eu(1) – O(7)	2.421(3)
Eu(1) – O(8)	2.381(3)

Table S8. ORTEP drawing (ellipsoids at 50% probability), selected distances (Å) of **2-b** at 93 K. All hydrogens of the ligands were omitted for clarity.

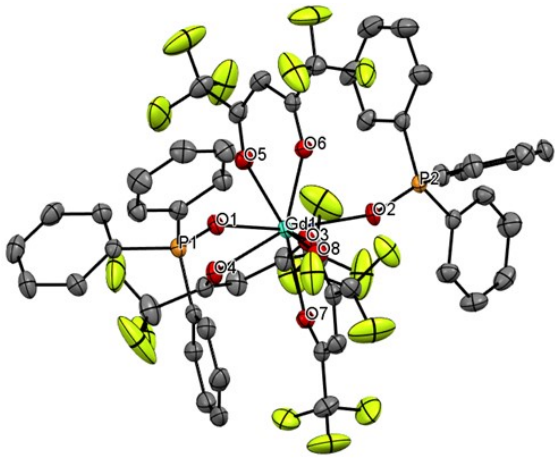

	Distance (Å)
Arsine oxide	
Gd(1) – O(1)	2.296(2)
Gd(1) – O(2)	2.295(2)
Hfa	
Gd(1) – O(3)	2.415(2)
Gd(1) – O(4)	2.414(2)
Gd(1) – O(5)	2.365(2)
Gd(1) – O(6)	2.441(2)
Gd(1) – O(7)	2.370(2)
Gd(1) – O(8)	2.424(2)

Table S9. ORTEP drawing (ellipsoids at 50% probability), selected distances (Å) of **3-a** at 93 K. All hydrogens of the ligands were omitted for clarity.

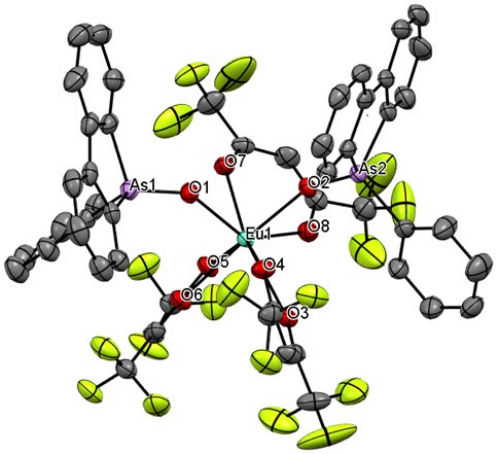

	Distance (Å)
Arsine oxide	
Eu(1) – O(1)	2.274(3)
Eu(1) – O(2)	2.283(3)
Hfa	
Eu(1) – O(3)	2.430(3)
Eu(1) – O(4)	2.388(4)
Eu(1) – O(5)	2.434(3)
Eu(1) – O(6)	2.422(3)
Eu(1) – O(7)	2.389(3)
Eu(1) – O(8)	2.432(3)

Table S10. ORTEP drawing (ellipsoids at 50% probability), selected distances (Å) of **3-b** at 93 K. All hydrogens of the ligands were omitted for clarity.

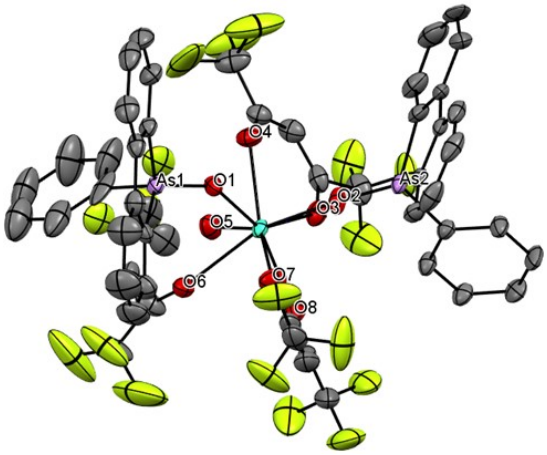

	Distance (Å)
Arsine oxide	
Gd(1) – O(1)	2.258(3)
Gd(1) – O(2)	2.253(4)
Hfa	
Gd(1) – O(3)	2.445(4)
Gd(1) – O(4)	2.463(4)
Gd(1) – O(5)	2.370(3)
Gd(1) – O(6)	2.460(4)
Gd(1) – O(7)	2.450(3)
Gd(1) – O(8)	2.383(4)

Table S11. ORTEP drawing (ellipsoids at 50% probability), selected distances (Å) of **4-a** at 93 K. All hydrogens of the ligands were omitted for clarity.

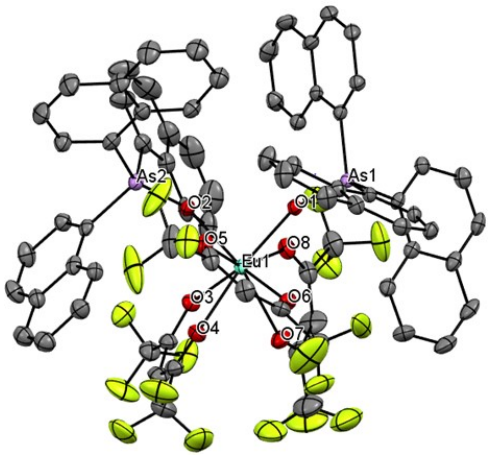

	Distance (Å)
Arsine oxide	
Eu(1) – O(1)	2.292(3)
Eu(1) – O(2)	2.279(3)
Hfa	
Eu(1) – O(3)	2.438(3)
Eu(1) – O(4)	2.399(3)
Eu(1) – O(5)	2.456(3)
Eu(1) – O(6)	2.388(3)
Eu(1) – O(7)	2.434(3)
Eu(1) – O(8)	2.448(3)

Table S12. ORTEP drawing (ellipsoids at 50% probability), selected distances (Å) of **4-b** at 93 K. All hydrogens of the ligands were omitted for clarity.

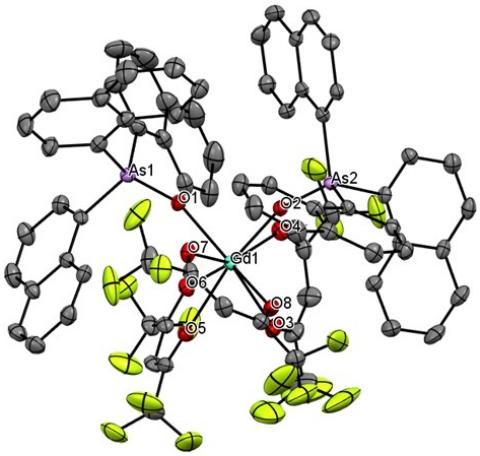

	Distance (Å)
Arsine oxide	
Gd(1) – O(1)	2.268(3)
Gd(1) – O(2)	2.290(4)
Hfa	
Gd(1) – O(3)	2.434(4)
Gd(1) – O(4)	2.441(4)
Gd(1) – O(5)	2.398(4)
Gd(1) – O(6)	2.436(3)
Gd(1) – O(7)	2.430(4)
Gd(1) – O(8)	2.389(3)

(a)

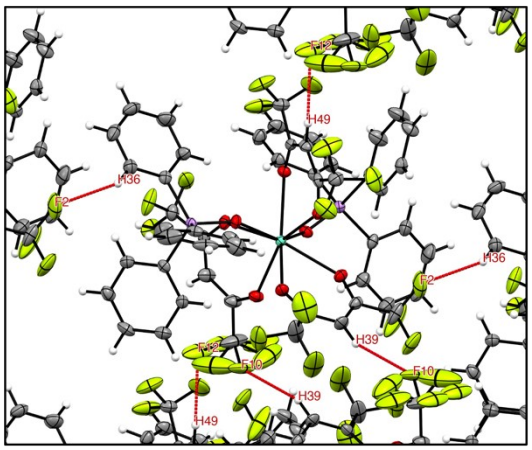

6 Inter-CH/F interactions

CH/F interaction	CH-F distance (Å)
H49 / F12 ×2	2.619
H36 / F2 ×2	2.531
H39 / F10 ×2	2.575

(b)

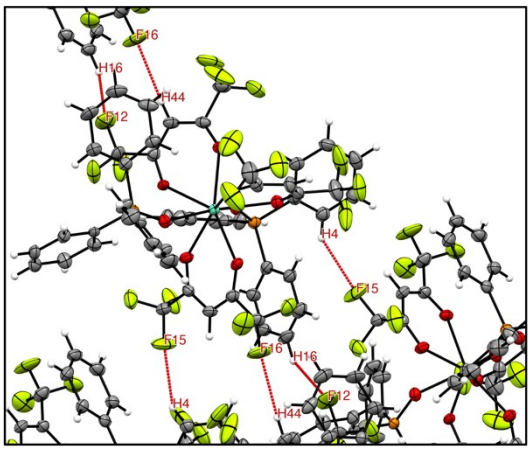

6 Inter-CH/F interactions

CH/F interaction	CH-F distance (Å)
H44 / F16 ×2	2.587
H16 / F12 ×2	2.637
H4 / F15 ×2	2.477

(c)

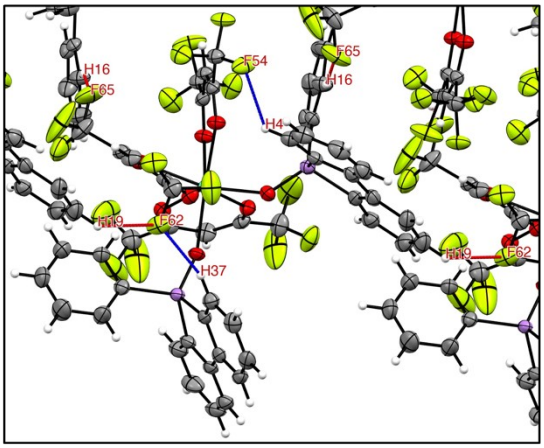

4 Inter-CH/F interactions
2 Intra-CH/F interactions

CH/F interaction	CH-F distance (Å)
H4 / F54	2.477
H37 / F62	2.433
H16 / F65 ×2	2.512
H19 / F62 ×2	2.636

(d)

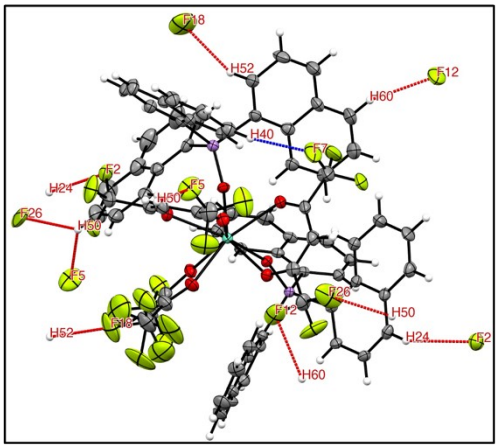

10 Inter-CH/F interactions
1 Intra-CH/F interaction

CH/F interaction	CH-F distance (Å)
H40 / F7	2.430
H24 / F2 ×2	2.668
H50 / F26 ×2	2.480
H50 / F5 ×2	2.530
H52 / F18 ×2	2.541
H60 / F12 ×2	2.638

Figure S3. CH/F interactions (intermolecular: red line, intramolecular: blue line) of (a)**1-a**, (b) **2-a**, (c) **3-a**, and (d) **4-a**. The CH/F distance is in the range of 2.430-2.668 Å being shorter than the sum of the van der Waals radii of H and F atoms (2.67 Å).

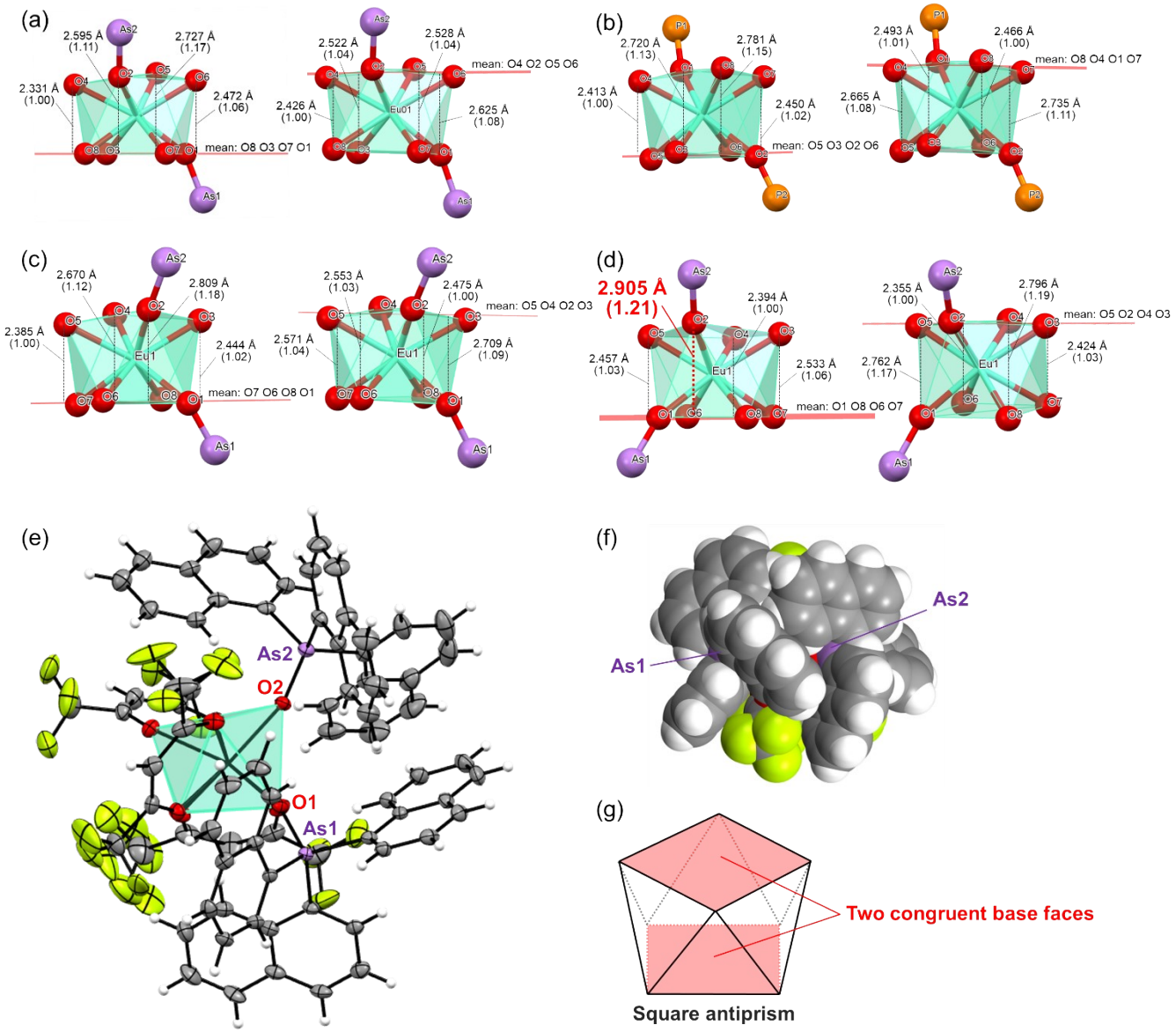

Figure S4. Distance between the least-squares plane (pink label) and oxygen atoms in the single crystal X-ray structure of (a) **1-a**, (b) **2-a**, (c) **3-a**, and (d) **4-a** (Inside parentheses: Ratio to minimum distance), and (e) ORTEP drawing (ellipsoids at 50% probability) the polyhedron composed of oxygen atoms of **4-a**, (f) Space–filling model (CPK model) of **4-a**, and (g) Ideal square antiprism (8-SAP) with two congruent base faces.

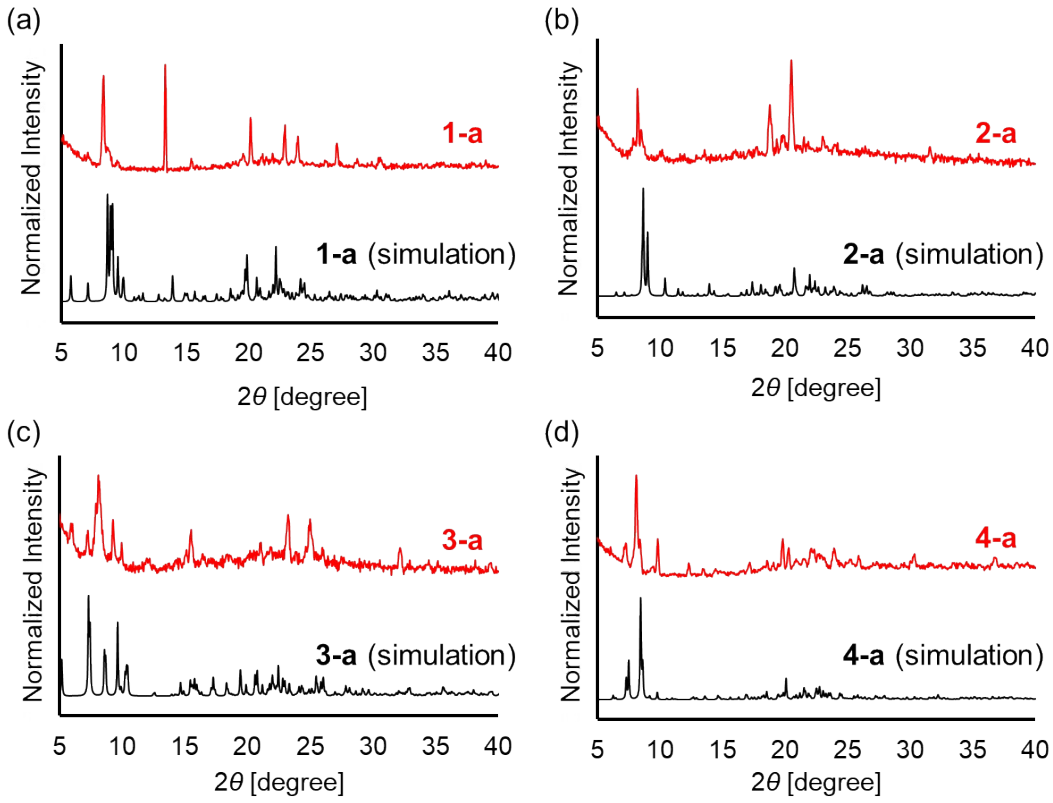

Figure S5. Powder X-ray diffraction pattern of (a) **1-a**, (b) **2-a**, (c) **3-a**, and (d) **4-a**.

3. Shape measure calculation

The continuous shape factor *S* was calculated to determine the coordination geometry of Eu^{3+} ion from the crystal data.

Table S13. Continuous shape measure factor *S* [a] for **1-a**, **1-b**, **2-a**, **2-b**, **3-a**, **3-b**, **4-a**, and **4-b**.

	S_{SAP} (D_{4d})	S_{TDH} (D_{2d})	S_{JBTPR} (C_{2v})	S_{BTPR} (C_{2v})
1-a	0.574	1.809	1.916	1.517
1-b	0.473	2.054	1.919	1.546
2-a	0.879	1.125	1.975	1.527
2-b	0.862	1.096	1.955	1.542
3-a	0.812	1.184	1.775	1.395
3-b	2.108	0.807	1.720	1.336
4-a	0.594	2.319	2.271	1.958
4-b	0.540	2.123	2.243	1.892

[a] Estimated by software SHAPE version 2.1. [10]

4. Photophysical properties

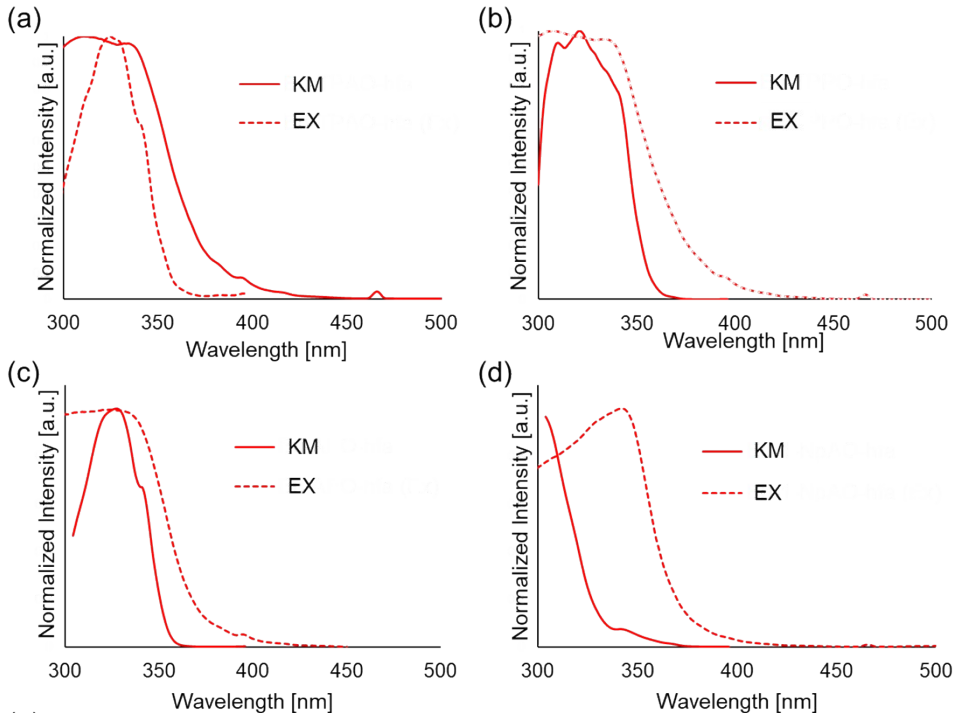

Figure S6. Diffuse reflection (the Kubelka-Munk calibration, solid line) and excitation (dashed line, monitored at 619 nm) spectra of (a) **1-a**, (b) **2-a**, (c) **3-a**, and (d) **4-a** in the solid state at 298 K. The maximum peak at 465 nm is attributed to the f-f transitions of Eu^{3+}-center ($^7F_0 \rightarrow {}^5D_2$). Diffuse reflection measurement samples were 10 wt% Eu^{3+} complexes dopes into SiO_2.

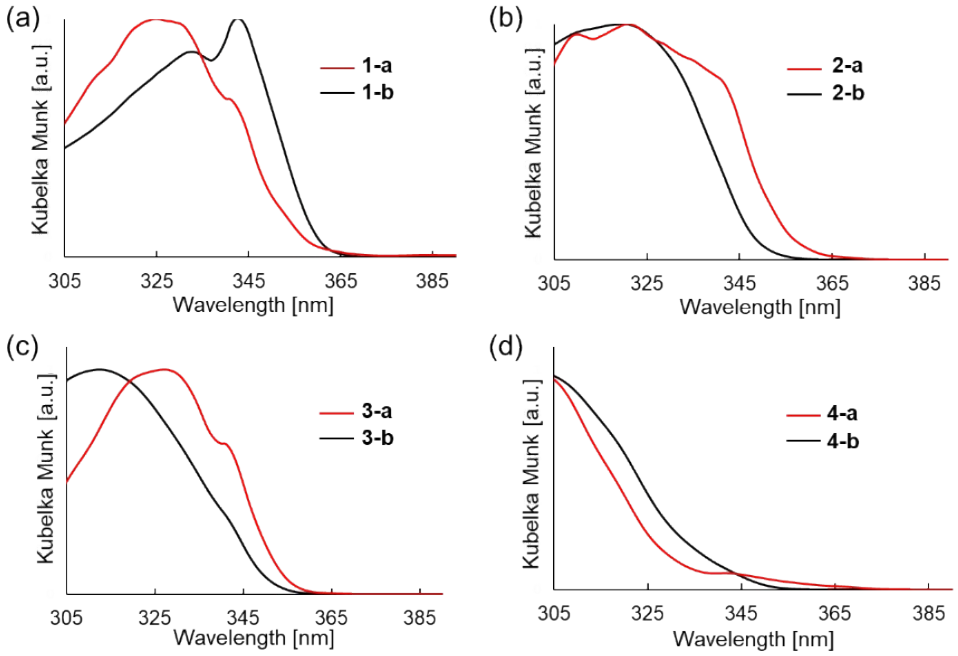

Figure S7. Diffuse reflection spectra (the Kubelka-Munk calibration) of (a) **1-a** and **1-b**, (b) **2-a** and **2-b**, (c) **3-a** and **3-b**, and (d) **4-a** and **4-b** in the solid state at 298 K. The measurement samples were 10 wt% Ln^{3+} complexes doped into SiO_2.

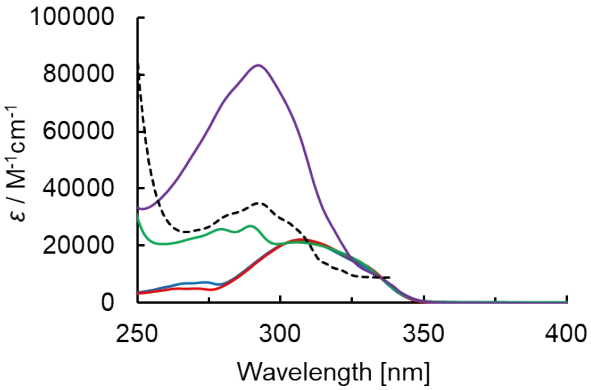

Figure S8. Electronic absorption spectra of **1-a** (red line), **2-a** (blue line), **3-a** (green line), **4-a** (purple line), and **4** (black broken line) in 1.0×10^{-5} M CH_2Cl_2 solution.

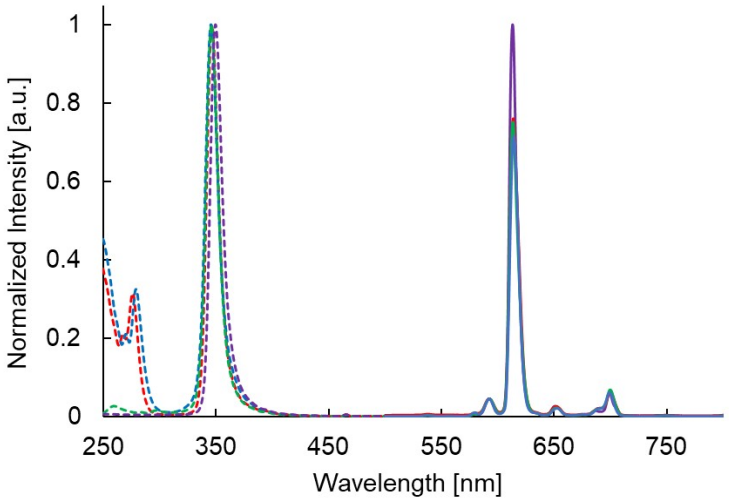

Figure S9. Luminescence (solid line) and excitation (broken line) spectra of **1-a** (red line), **2-a** (blue line), **3-a** (green line), and **4-a** (purple line) at 298 K in 1.0×10^{-3} M CH_2Cl_2 solution.

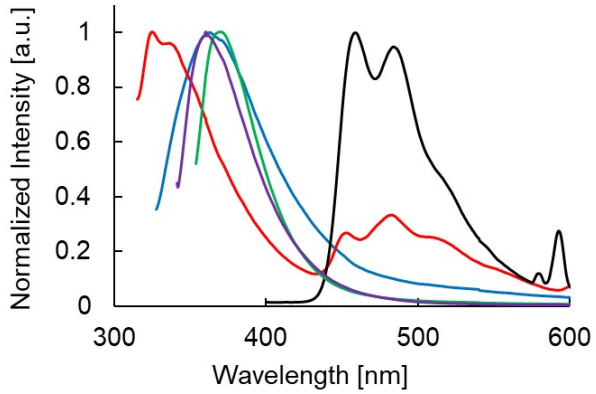

Figure S10. Luminescence (solid line) spectra of **1** (red line), **2** (blue line), **3** (green line), **4** (purple line), $[Gd(hfa)_3(H_2O)_2]$ (black line) at 298 K in solid state.

Table S14. Photophysical properties of Eu^{3+} complexes in CH_2Cl_2 at 298 K.

	I_{ED}/I_{MD}[c,d]	τ_{obs}[e,i] [ms]	Φ_{tot}[f,i] [%]	$\Phi_{f\text{-}f}$[c,i] [%]	k_r[g] [$10^2 \times s^{-1}$]	k_{nr}[g] [$10^2 \times s^{-1}$]	η_{sens}[h]
1-a[a]	17.5	0.75	56	66	8.7	4.6	0.86
2-a[a]	16.6	0.82	53	64	7.8	4.4	0.84
3-a[a]	15.8	0.73	52	61	8.3	5.4	0.85
4-a[b]	20.6	0.72	61	72	10.0	3.9	0.84

[a] I_{614}/I_{593}: 1.0×10^{-3} M CH_2Cl_2 solution, τ_{tot}, $\tau_{f\text{-}f}$, $\Phi_{f\text{-}f}$, and Φ_{tot}: 1.0×10^{-2} M CH_2Cl_2 solution, [b] I_{614}/I_{593}: 1.0×10^{-3} M CH_2Cl_2 solution, τ_{tot}, $\tau_{f\text{-}f}$, $\Phi_{f\text{-}f}$, and Φ_{tot}: saturated concentration CH_2Cl_2 solution (< 1.0×10^{-2} M), [c] Excited at 465 nm. [d] Relative intensity of $^5D_0 \rightarrow {}^7F_2$ transition (electric dipole) to $^5D_0 \rightarrow {}^7F_1$ (magnetic dipole). [e] Excited at 340 nm (monitored at 614 nm). [f] Excited at 335 nm. [g] Calculated using equations 2-6 in the experimental section. $^5D_0 \rightarrow {}^7F_5$, and $^7F_6$ transitions were not considered in the calculation of the intrinsic quantum yields because the transition emission was very noisy owing to the weak emission intensity. [h] $\eta_{sens} = \Phi_{tot}/\Phi_{f\text{-}f}$. [i] It was confirmed that Φ_{tot}, τ_{obs}, and $\Phi_{f\text{-}f}$ were reproducible within 1% errors in five measurements.

Table S15. Photophysical properties of Eu^{3+} complexes under air and Ar atmosphere at 298 K in the solid state.

	Atom.	τ_{obs}[c,g] [ms]	Φ_{tot}[d,g] [%]	$\Phi_{f\text{-}f}$[a,e,g] [%]	k_r[e] [$10^2 \cdot s^{-1}$]	k_{nr}[e] [$10^2 \cdot s^{-1}$]	η_{sens}[f]
1-a	air	0.65	54	64	9.9	5.5	0.84
	Ar	0.67	56	64	9.7	5.3	0.86
2-a	air	0.76	54	62	8.2	4.9	0.87
	Ar	0.78	56	63	8.1	4.7	0.88
3-a	air	0.79	51	66	8.4	4.2	0.76
	Ar	0.77	50	64	8.3	4.7	0.79
4-a	air	0.65	65	74	11.4	4.1	0.88
	Ar	0.65	69	74	11.4	4.0	0.93

Measured using tubes filled with Ar gas. [a] Excited at 465 nm. [b] Relative intensity of $^5D_0 \rightarrow {}^7F_2$ transition (electric dipole) to $^5D_0 \rightarrow {}^7F_1$ (magnetic dipole). [c] Excitation at 335 nm (monitored at 614 nm). [d] Excited at λ_{ex}. [e] Calculated using equations 2-6 in the experimental section. $^5D_0 \rightarrow {}^7F_5$, and $^7F_6$ transitions were not considered in the calculation of the intrinsic quantum yields because the transition emission was very noisy owing to the weak emission intensity. [f] $\eta_{sens} = \Phi_{tot}/\Phi_{f\text{-}f}$. [g] It was confirmed that Φ_{tot}, τ_{obs}, and $\Phi_{f\text{-}f}$ were reproducible within 1% errors in five measurements.

Table S16. Photophysical properties of Gd^{3+} complexes in the solid state at 77 K.

	λ_{ex}[a] [nm]	λ_{em}[a] [nm]	Φ_{PL}[c] [%]	τ [d,e] [ms]
1-b	336	464	48	4.0
2-b	335	464	64	7.8
3-b	335	508	14	2.7
4-b	335	554	7.1	57

[a] Excitation maximum (emission at λ_{em}). [b] Excited at λ_{ex}. [c] Emission quantum yield. [d] Emission lifetime. [e] Excited at 340 nm (monitored at λ_{em}).

Table S17. Optical properties of Eu^{3+} complexes in CH_2Cl_2.

	ε_{306}[a] [$M^{-1}cm^{-1}$]	ε_L[b] [$M^{-1}cm^{-1}$]	Φ_{tot}[c] [%]	I_{306}[d] [$M^{-1}cm^{-1}$]	I_L[e] [$M^{-1}cm^{-1}$]
1-a	22,300	5,100	56	1.2×10^4	2.9×10^3
2-a	22,000	7,400	53	1.2×10^4	3.9×10^3
3-a	21,300	26,900	52	1.1×10^4	1.4×10^4
4-a	60,700	83,200	61	3.7×10^4	5.1×10^4

[a] Molar absorption coefficient attributed at absorption maxima of the hfa anion. [b] Molar absorption coefficient attributed at absorption maxima of the neutral ligands (**1-a**: 271 nm, **2-a**: 274 nm, **3-a**: 290 nm, **4-a**: 292 nm). [c] λ_{ex} = 335 nm. [d] $I_{306} = \varepsilon_{306}\times\Phi_{tot}$, $I_L = \varepsilon_L\times\Phi_{tot}$.

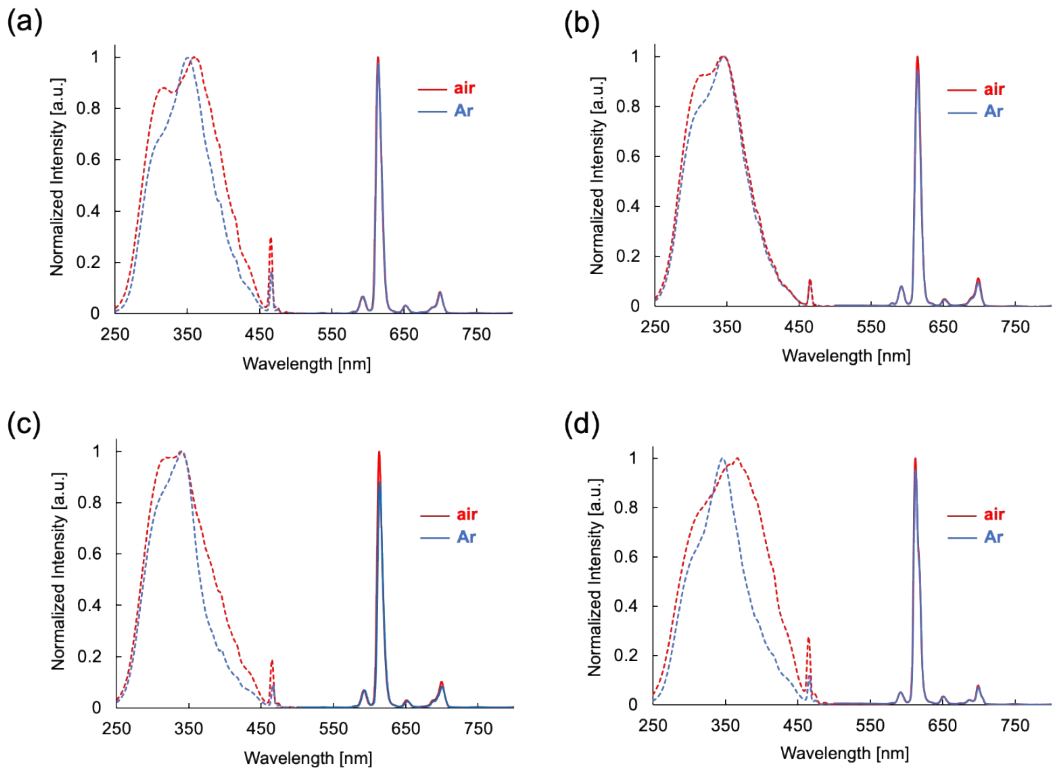

Figure S11. Luminescence (solid line) and excitation (broken line) spectra of (a) **1-a**, (b) **2-a**, (c) **3-a**, (d) **4-a** excited at 465 nm in the solid state at 298 K under air (red line) and Ar (blue line) atmosphere.

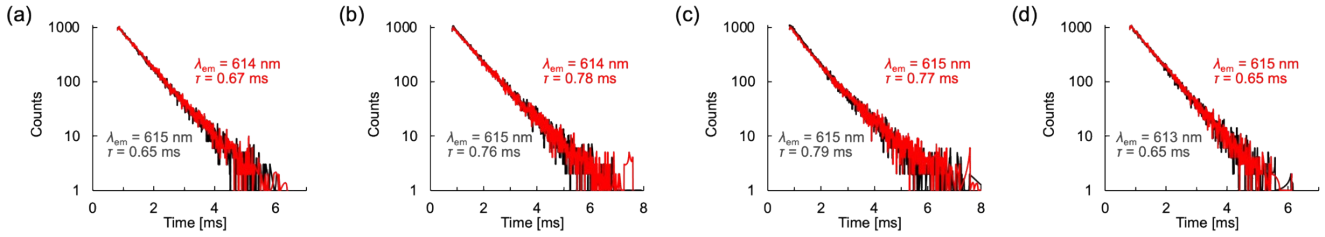

Figure S12. The emission decay kinetics of (a) **1-a**, (b) **2-a**, (c) **3-a**, and (d) **4-a** excited at 340 nm in the solid state under air (black line) and Ar atmosphere (red line) at 298 K. It was confirmed that τ_{obs} was reproducible within 1% errors in five measurements.

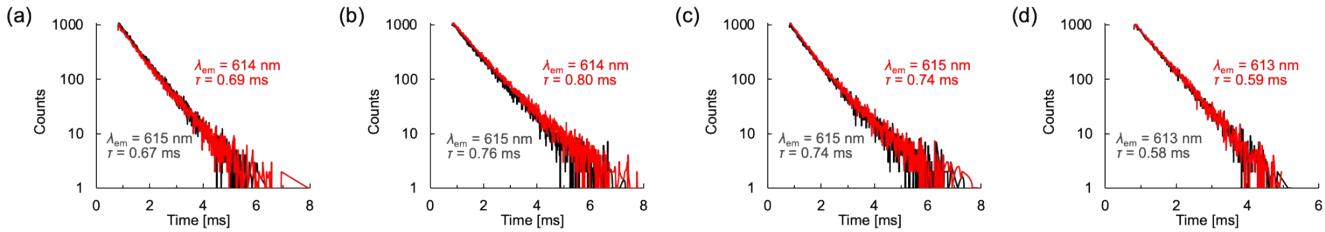

Figure S13. The emission decay kinetics of (a) **1-a**, (b) **2-a**, (c) **3-a**, and (d) **4-a** excited at 470 nm in the solid state under air (black line) and Ar atmosphere (red line) at 298 K. It was confirmed that τ_{obs} was reproducible within 1% errors in five measurements.

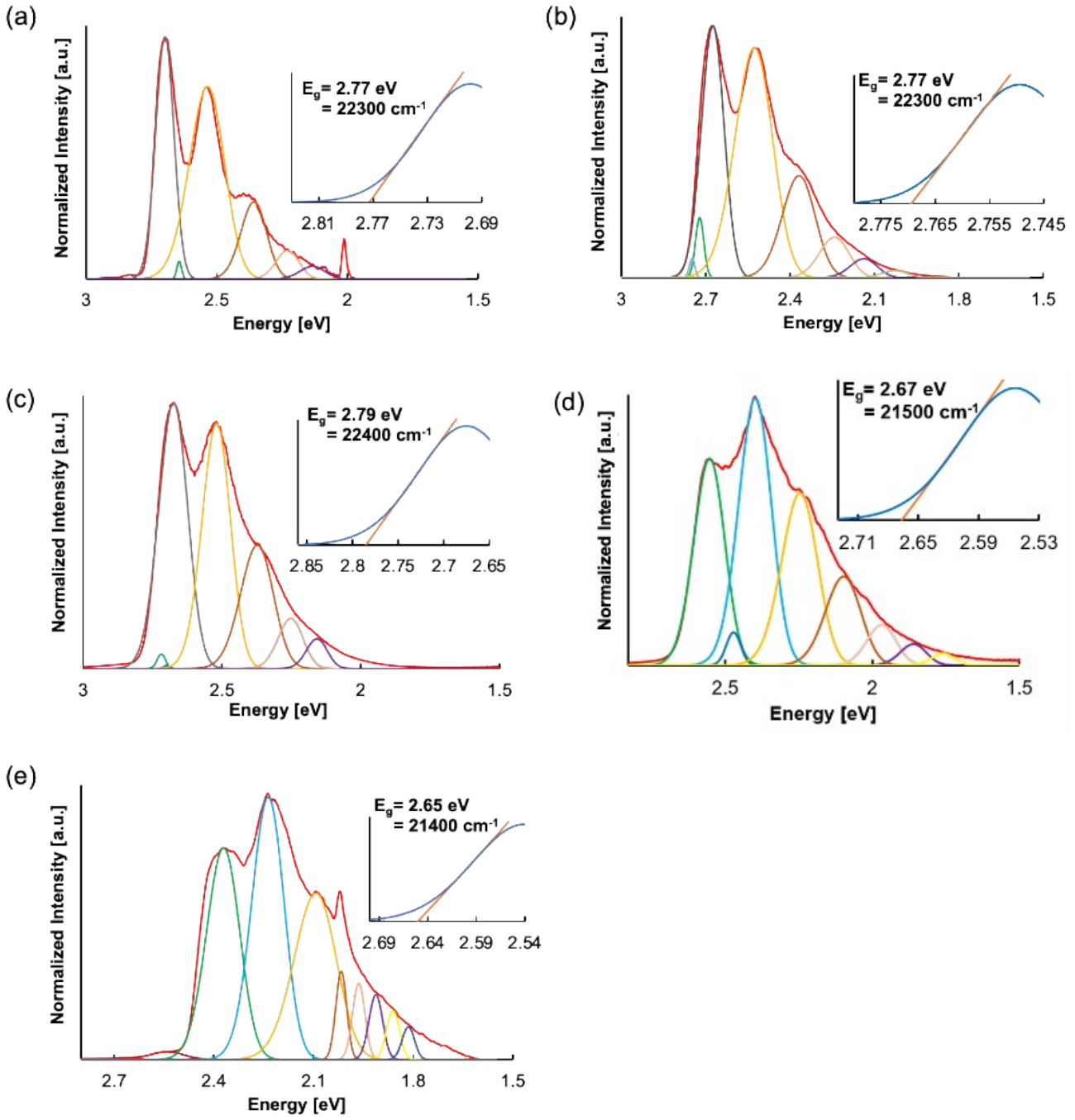

Figure S14. Gaussian band deconvolution of the phosphorescence spectra of (a) [Gd(hfa)$_3$(H_2O)$_2$], (b) **1-b**, (c) **2-b**, (d) **3-b**, and (e) **4-b** in the solid state at 77 K for the estimation of the T_1 energy levels (red line; original spectra, other colors line; deconvoluted spectra) in the solid state. Inset is the extrapolation (orange line) of the 0−0 transition band (blue line).

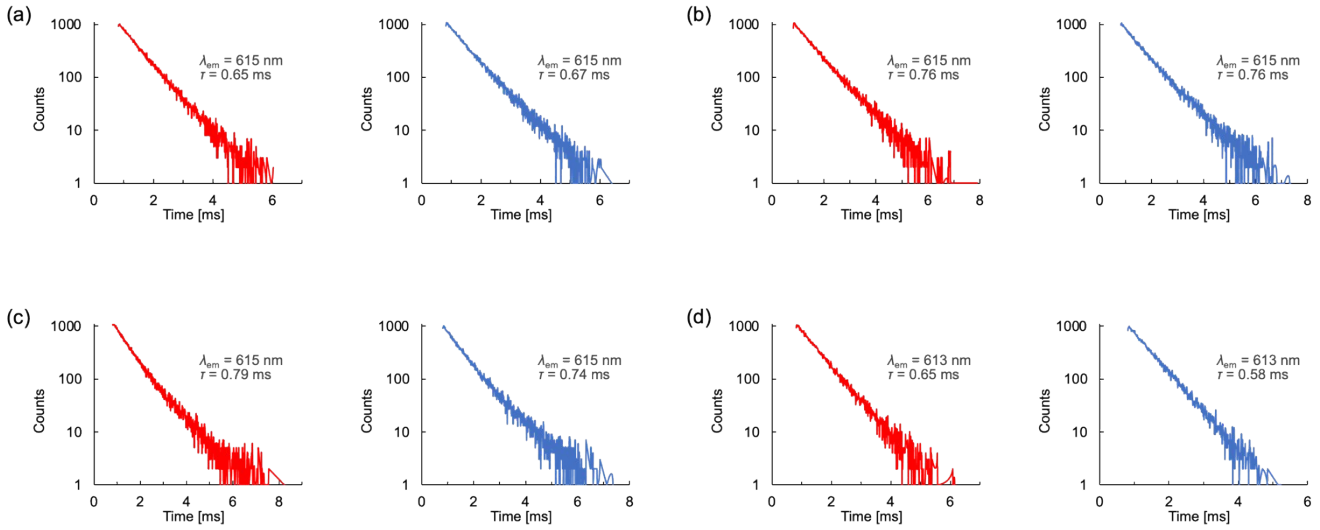

Figure S15. The emission decay kinetics of (a) **1-a**, (b) **2-a**, (c) **3-a**, and (d) **4-a** excited at 340 nm (red line) and 470 nm (blue line) in the solid state under air at 298 K. It was confirmed that τ_{obs} was reproducible within 1% errors in five measurements.

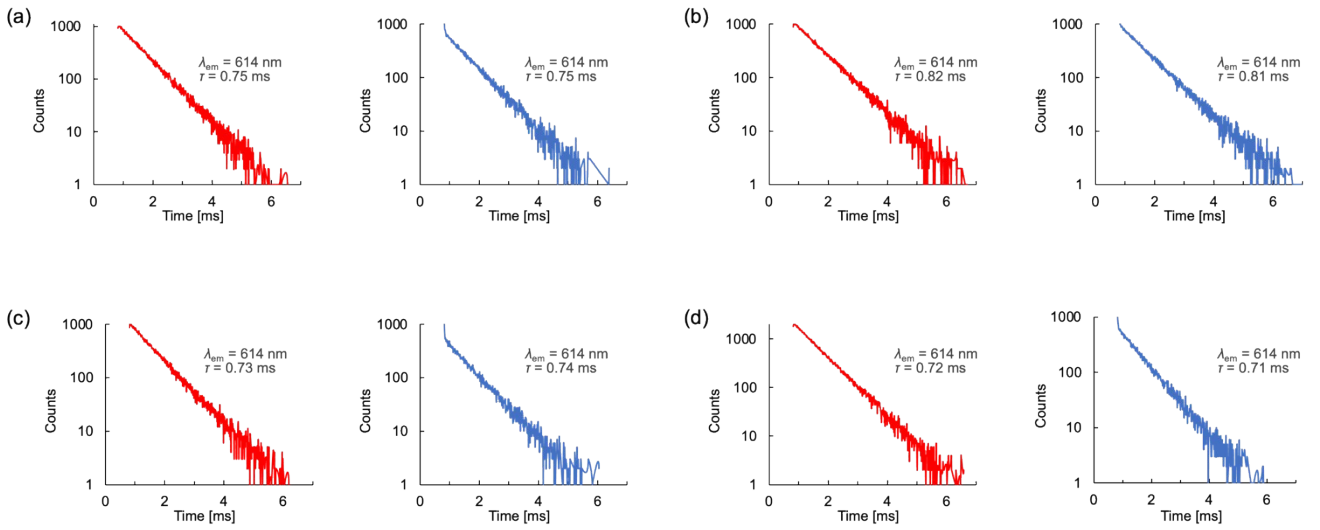

Figure S16. The emission decay kinetics of (a) **1-a**, (b) **2-a**, (c) **3-a**, and (d) **4-a** excited at 340 nm (red line) and 470 nm (blue line) in CH_2Cl_2 (**4-a**: 5.0×10^{-3} M, other solutions: 1.0×10^{-2} M) at 298 K. It was confirmed that τ_{obs} was reproducible within 1% errors in five measurements.

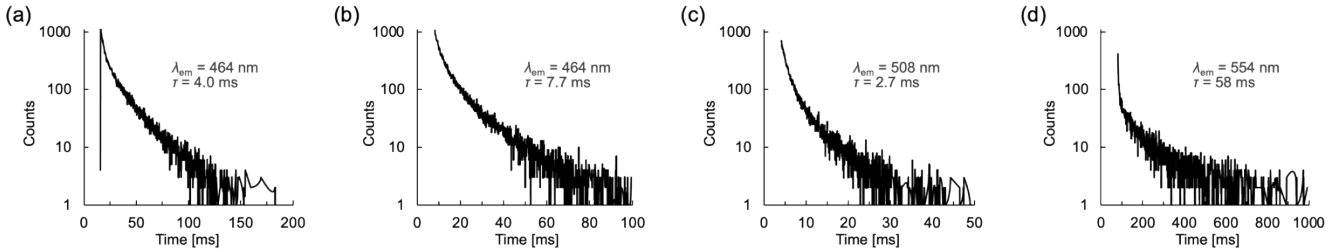

Figure S17. The emission decay kinetics of (a) **1-b**, (b) **2-b**, (c) **3-b**, and (d) **4-b** in the solid state under air at 77 K (λ_{ex} = 340 nm).

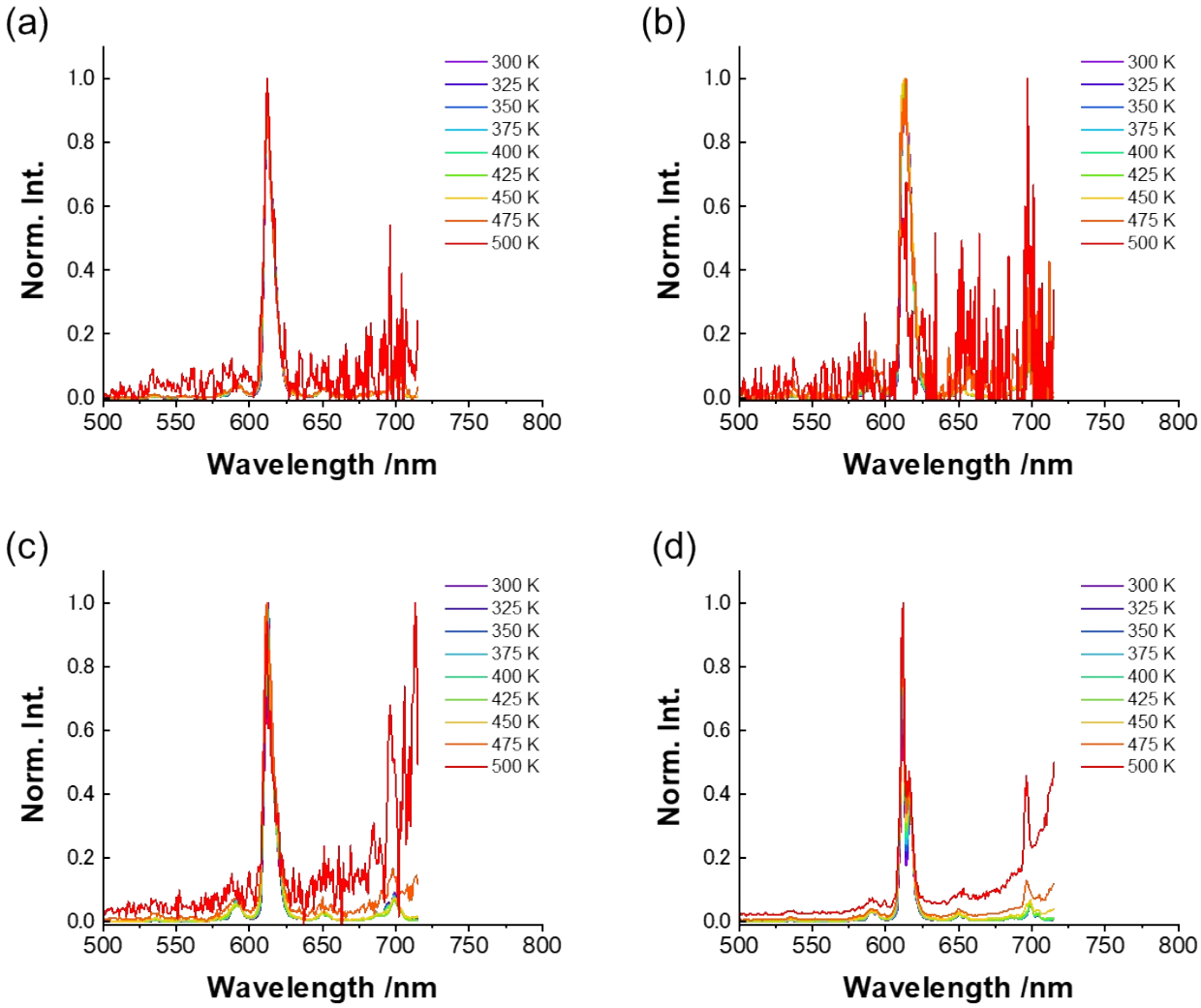

Figure S18. Variable temperature (VT) PL spectra of (a) **1-a**, (b) **2-a**, (c) **3-a**, and (d) **4-a** excited at 365 nm. The spectra were normalized by emission maxima at each temperature.

5. Thermal properties

Preparation
Eu^{3+} complex samples were dried in an 80 °C vacuum oven for 3 hours before thermogravimetric analysis was performed.

Table S18. Values of thermal degradation temperatures $T_{d5\%}$, $T_{d10\%}$, $T_{d20\%}$, and $T_{d40\%}$ of $[Eu(hfa)_3(H_2O)_2]$, **1-a**, **2-a**, **3-a**, and **4-a** under N_2 gas.

	$[Eu(hfa)_3(H_2O)_2]$	**1-a**	**2-a**	**3-a**	**4-a**
$T_{d5\%}$ [°C] [a]	176	240	247	244	284
$T_{d10\%}$ [°C] [a]	206	248	270	255	310
$T_{d20\%}$ [°C] [a]	217	264	286	266	325
$T_{d40\%}$ [°C] [a]	229	304	301	284	339

[a] Temperature at 5%, 10%, 20%, 40% weight loss obtained from thermogravimetric analysis (TGA), respectively.

6. Theoretical calculation

Computational method
Time-dependent density functional theory (TD-DFT) calculations to estimate dipole moment were carried out by B3LYP/6-31G+(d,p).Natural bonding orbital (NBO) analysis for natural population analysis (NPA) was carried out by B3LYP/6-31G+(d,p).[23] These calculations were based on the geometry of **1**, **2**, **3** and **4** within **1-a**, **2-a**, **3-a** and **4-a**, respectively (Table S20-S23). For these calculation, Gaussian 16 code was employed.[24]

Table S19. NPA and Dipole moment of arsine and phosphine ligands in Eu^{3+} complexes.

	NPA [a]		Dipole moment [b] [D]
	pnictogen	oxygen	
1	1.96	-1.10	5.08
2	2.03	-1.11	4.50
3	1.96	-1.07	5.60
4	1.98	-1.09	4.60

[a] Level of theory: (DFT)B3LYP/6-31G+(d,p). [b] Level of theory: (TD-DFT)B3LYP/6-31G+(d,p) for Pn=O bond (Pn = P, As).

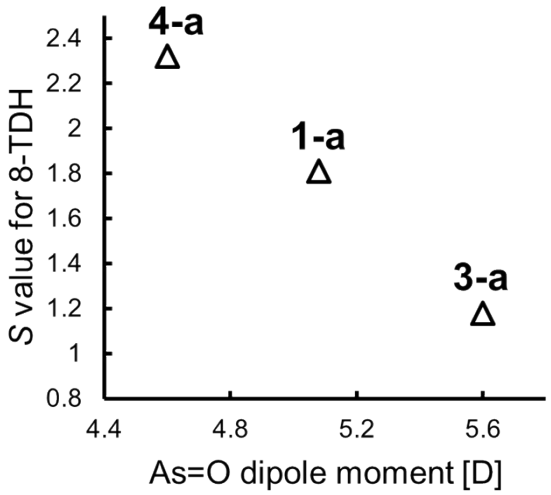

Figure S19. Correlation between As=O dipole moment and 8-TDH geometry degree.

Table S20. Atom coordinates and absolute energy levels for **1**.

1: *E*(B3LYP) = -3003.76858949 A.U.

Center Number	Atomic Number	Atomic Type	Coordinate		
			X	Y	Z
1	33	0	0.010259	-0.054301	0.69169
2	8	0	-0.088884	-0.189485	-2.344361
3	6	0	-0.342563	1.741225	-0.110623
4	6	0	-1.445223	2.398684	-0.65686
5	1	0	-1.99001	1.967523	-1.305079
6	6	0	-1.351982	-1.20701	0.017282
7	6	0	2.725051	-0.685215	-1.108372
8	1	0	2.507113	-0.50534	-2.015914
9	6	0	0.455005	2.351729	0.834745
10	1	0	1.208491	1.898275	1.19321
11	6	0	-1.733015	3.684727	-0.241223
12	1	0	-2.47248	4.148553	-0.616397
13	6	0	1.757852	-0.560851	-0.114054
14	6	0	-0.950418	4.298426	0.715839
15	1	0	-1.161228	5.177392	1.00698
16	6	0	-1.484612	-1.474646	1.371072
17	1	0	-0.87822	-1.10887	2.004107
18	6	0	0.1428	3.636747	1.256308
19	1	0	0.678007	4.064377	1.914175
20	6	0	2.090578	-0.805456	1.208481
21	1	0	1.434101	-0.714842	1.889214
22	6	0	4.003944	-1.073945	-0.761759
23	1	0	4.666381	-1.171731	-1.435218
24	6	0	-2.539362	-2.298569	1.774741
25	1	0	-2.640209	-2.509575	2.696077
26	6	0	-3.426253	-2.805201	0.869482
27	1	0	-4.140935	-3.356258	1.166289
28	6	0	4.326867	-1.318802	0.553888
29	1	0	5.209615	-1.586126	0.783108
30	6	0	-2.250598	-1.718951	-0.888919
31	1	0	-2.156672	-1.519778	-1.813583
32	6	0	3.382339	-1.179839	1.533431
33	1	0	3.613855	-1.341577	2.440632
34	6	0	-3.292733	-2.525331	-0.46015
35	1	0	-3.911336	-2.880542	-1.086776

Table S21. Atom coordinates and absolute energy levels for **2**.

2: *E*(B3LYP) = -1111.27090421 A.U.

Center Number	Atomic Number	Atomic Type	Coordinate		
			X	Y	Z
1	15	0	-0.017333	0.039524	837138
2	8	0	-0.048056	-0.123234	2.32389
3	6	0	1.463808	-0.841196	0.198001
4	6	0	2.546779	-0.996866	1.062509
5	1	0	2.493887	-0.698464	1.941323
6	6	0	-1.458371	-0.851333	0.174098
7	6	0	-1.03289	2.504516	0.663806
8	1	0	-1.707125	2.180793	1.215332
9	6	0	-0.006069	1.656037	0.243644
10	6	0	3.698456	-1.598303	0.598534
11	1	0	4.42235	-1.704555	1.172528
12	6	0	-2.009142	-0.527554	-1.057761
13	1	0	-1.622712	0.14614	-1.568877
14	6	0	3.792822	-2.0407	-0.700589
15	1	0	4.573328	-2.449823	-0.997949
16	6	0	-2.058707	-1.845269	0.937875
17	1	0	-1.707994	-2.073354	1.768585
18	6	0	2.722363	-1.878019	-1.56672
19	1	0	2.78793	-2.168158	-2.448208
20	6	0	1.556722	-1.282866	-1.115401
21	1	0	0.834812	-1.179291	-1.693077
22	6	0	-1.046357	3.829995	0.25692
23	1	0	-1.729923	4.395995	0.536566
24	6	0	0.999447	2.15762	-0.559384
25	1	0	1.693642	1.602046	-0.833908
26	6	0	-3.707235	-2.180342	-0.772832
27	1	0	-4.45386	-2.634107	-1.092728
28	6	0	-3.119859	-1.188127	-1.53218
29	1	0	-3.473564	-0.966684	-2.3627
30	6	0	-3.184125	-2.495633	0.452954
31	1	0	-3.589627	-3.154931	0.966981
32	6	0	0.979128	3.483846	-0.958903
33	1	0	1.660337	3.817997	-1.497508
34	6	0	-0.04841	4.306481	-0.559815
35	1	0	-0.067196	5.191411	-0.843081

Table S22. Atom coordinates and absolute energy levels for **3**.

3: *E*(B3LYP) = -3002.52587720 A.U.

Center Number	Atomic Number	Atomic Type	Coordinate		
			X	Y	Z
1	33	0	-0.348523	0.089667	0.890829
2	8	0	0.571767	-0.300887	2.51508
3	6	0	2.031244	-0.022182	-0.024904
4	6	0	-2.910931	1.660386	-0.762108
5	1	0	-3.65877	1.329888	-1.205172
6	6	0	-0.804157	1.336937	0.351692
7	6	0	-1.971866	-0.685196	-0.371823
8	6	0	3.199824	-0.377726	0.619366
9	1	0	3.176828	-0.668607	1.502262
10	6	0	-3.037796	-1.443802	-0.85774
11	1	0	-3.797137	-1.026566	-1.196028
12	6	0	-0.86297	-1.371906	0.134842
13	6	0	-1.934782	0.785147	-0.295026
14	6	0	-0.647704	2.686292	0.528712
15	1	0	0.111126	3.025169	0.947031
16	6	0	4.396181	-0.299759	-0.048061
17	1	0	5.185264	-0.527932	0.388949
18	6	0	-2.765992	3.027412	-0.56383
19	1	0	-3.431979	3.605012	-0.861544
20	6	0	-0.77066	-2.726679	0.14936
21	1	0	-0.009129	-3.148168	0.476503
22	6	0	-1.651111	3.547174	0.066726
23	1	0	-1.567321	4.465534	0.184241
24	6	0	-2.95041	-2.825077	-0.829427
25	1	0	-3.661903	-3.330107	-1.151879
26	6	0	2.061086	0.38347	-1.340572
27	1	0	1.273382	0.618744	-1.776226
28	6	0	4.43681	0.114231	-1.367883
29	1	0	5.251015	0.171656	-1.812645
30	6	0	-1.841725	-3.46926	-0.33632
31	1	0	-1.807569	-4.39819	-0.32764
32	6	0	3.283599	0.439062	-2.015893
33	1	0	3.30897	0.698531	-2.908506

Table S23. Atom coordinates and absolute energy levels for **4**.

4: *E*(B3LYP) = -3464.62627600 A.U.

Center Number	Atomic Number	Atomic Type	Coordinate		
			X	Y	Z
1	33	0	0.078619	-0.026686	-0.412225
2	8	0	0.195058	0.104695	-2.062435
3	6	0	1.805876	0.235565	0.380966
4	6	0	-0.574203	-1.734181	0.203644
5	6	0	2.884366	-1.405345	-1.186693
6	1	0	2.049477	-1.605197	-1.592847
7	6	0	0.17313	-2.402619	1.131054
8	1	0	1.0262	-2.068378	1.380291
9	6	0	-1.147863	1.293296	0.262572
10	6	0	1.927715	1.126316	1.412274
11	1	0	1.158499	1.584822	1.729618
12	6	0	-1.036044	2.67191	-0.116343
13	6	0	-3.881627	-2.052464	-1.484789
14	1	0	-4.410827	-1.607741	-2.135903
15	6	0	-2.194947	0.866635	1.031688
16	1	0	-2.237812	-0.043893	1.297818
17	6	0	4.014482	-2.026138	-1.629251
18	1	0	3.95651	-2.657996	-2.336238
19	6	0	2.940728	-0.465685	-0.128273
20	6	0	-2.066058	3.557861	0.307679
21	6	0	-3.213891	1.755636	1.435378
22	1	0	-3.935972	1.44247	1.967378
23	6	0	-1.844953	-2.217054	-0.208739
24	6	0	0.058262	3.185488	-0.841168
25	1	0	0.736616	2.598373	-1.154444
26	6	0	-1.949246	4.930273	-0.013888
27	1	0	-2.643389	5.529523	0.235218
28	6	0	-3.157842	3.064523	1.06206
29	1	0	-3.861301	3.653687	1.309228
30	6	0	4.280607	0.73012	1.531765
31	1	0	5.126875	0.910158	1.923912
32	6	0	3.18543	1.372503	2.010521
33	1	0	3.262196	1.979748	2.736836
34	6	0	-0.320259	-3.59036	1.719656
35	1	0	0.211683	-4.07142	2.343452
36	6	0	-2.650812	-1.569836	-1.17384

37	1	0	-2.327463	-0.789644	-1.608101
38	6	0	5.262831	-1.745786	-1.049929
39	1	0	6.045699	-2.17425	-1.376126
40	6	0	-3.632197	-3.853675	0.075304
41	1	0	-3.981714	-4.629684	0.498088
42	6	0	4.203141	-0.19593	0.472082
43	6	0	-2.348945	-3.395625	0.420995
44	6	0	-4.379513	-3.200536	-0.854259
45	1	0	-5.243805	-3.524514	-1.078684
46	6	0	-1.553762	-4.03636	1.389122
47	1	0	-1.894364	-4.808423	1.826001
48	6	0	5.349579	-0.862262	-0.030638
49	1	0	6.197905	-0.684619	0.359376
50	6	0	-0.86479	5.407567	-0.672323
51	1	0	-0.78774	6.336843	-0.848715
52	6	0	0.14679	4.524287	-1.092573
53	1	0	0.901919	4.864484	-1.557595

7. Photograph

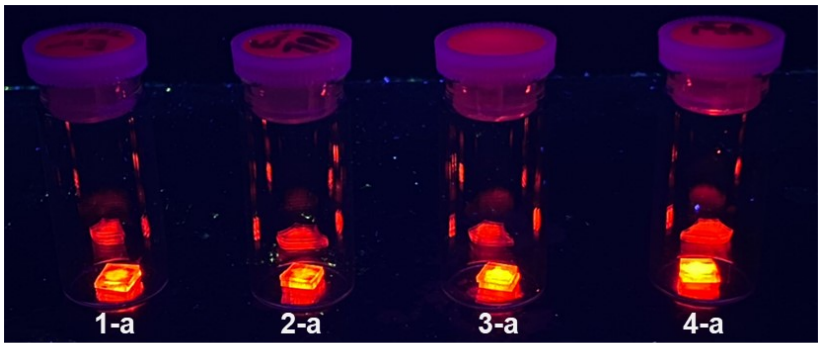

Figure S20. Photographs of **1-a**, **2-a**, **3-a**, and **4-a** in solid state under black light irradiation. Eu^{3+} samples were placed between KBr plates and photograph was taken.

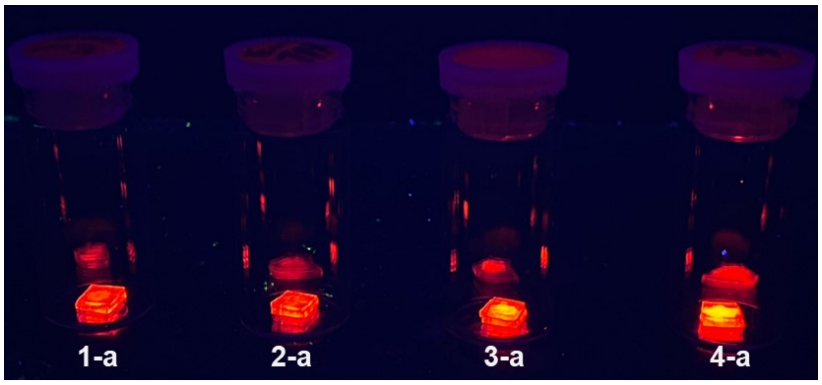

Figure S21. Photographs of **1-a**, **2-a**, **3-a**, and **4-a** in solid state under UV light irradiation. Eu^{3+} samples were placed between KBr plates and photograph was taken.

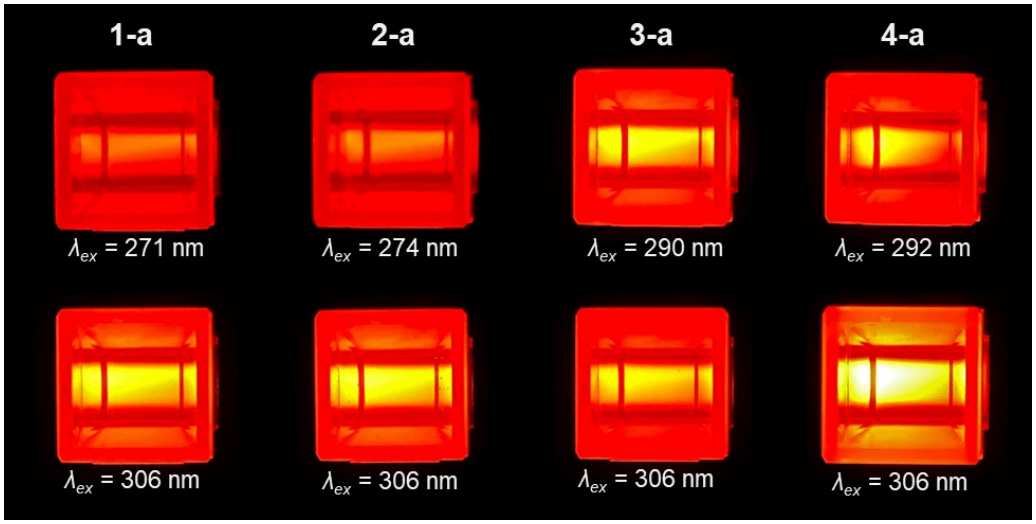

Figure S22. Photographs of **1-a**, **2-a**, **3-a**, and **4-a** in 1.0×10^{-5} M CH_2Cl_2 solution under excitation light (**1-a**: λ_{ex} = 271, 306 nm, **2-a**: λ_{ex} = 274, 306 nm, **3-a**: λ_{ex} = 290, 306 nm, **4-a**: λ_{ex} = 292, 306 nm) irradiation. Top view of quartz cell containing CH_2Cl_2 solution.

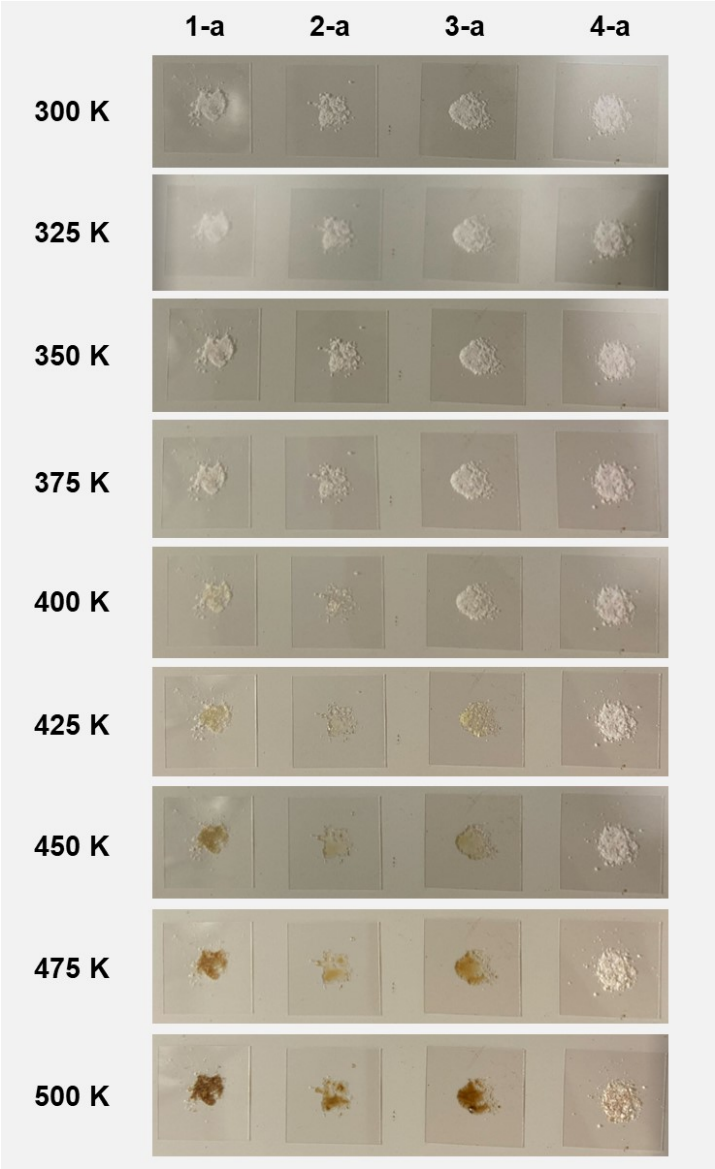

Figure S23. Photographs of solid samples of **1-a**, **2-a**, **3-a**, and **4-a** at various temperatures. These samples were heated using a hot plate under atmospheric conditions.

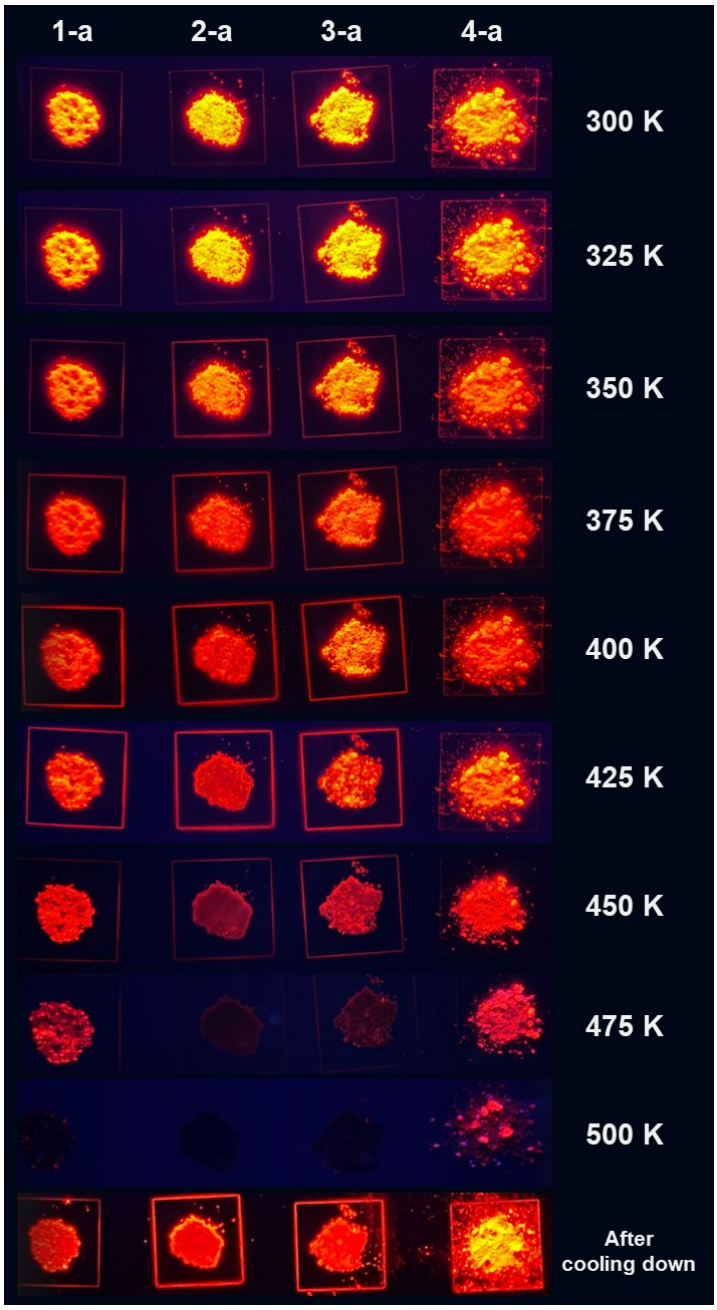

Figure S24. Photographs of solid samples of **1-a**, **2-a**, **3-a**, and **4-a** under UV lampirradiation (365 nm) at various temperatures. These samples were heated using a hot plate under atmospheric conditions.